Int J Adv Manuf Technol (2006) 27: 925–929
DOI 10.1007/s00170-004-2261-x

ORIGINAL ARTICLE

H.Y. Zheng · H. Liu · S. Wan · G.C. Lim · S. Nikumb · Q. Chen

Ultrashort pulse laser micromachined microchannels and their application in an optical switch

Received: 9 March 2004 / Accepted: 20 May 2004 / Published online: 9 February 2005

Abstract The capability of direct writing makes ultrashort pulse laser significant in the microfabrication of MEMS devices based on polymer and glass. In particular, nanosecond and femtosecond lasers are able to transfer the adequate energy in femtosecond intervals for the removal of the materials. Because of its advantages, just like the small feature size, smooth finishing surface, flexible structuring and the minimum thermal effect, ultrashort pulse lasers have become a convincing technique with the high peak power. This paper presents the femtosecond laser machining results of the polycarbonate, aluminosilicate glasses and nanosecond laser machining of aluminosilicate glasses. The microchannels with the critical micron-scale dimensions and the sub-micron scale surface roughness were achieved by the optimized operating parameters of the laser. The major influence factors such as cutting speed, power energy, and power stability were analyzed to obtain the optimized parameters for the fabrication of the microchannels for a bubble switch. The ultrashort pulse laser micromachining was applied in the prototype of a bubble optical switch. By miniaturization of the structure of the microchannel, the switch speed can be promisingly improved.

Keywords Bubble optical switch · Femtosecond laser micromachining · Microchannel · Surface roughness · Ultrashort pulse laser

1 Introduction

The great demand for the communication bandwidth urges to develop an all-optical network to make the signals stay in optical form throughout the network. To achieve it, it is inevitable to get a replacement for the current switches, which have to convert optical signals into electrical signals and then back into optical form for further transmission. The gains of avoiding signal conversion could not only significantly reduce costs but also move larger amount of data, voice, and video signals at higher speeds.

Several methods were reported for optical switching purposes. One of the methods is microfluidic based optical switching, which does not have moving mechanical parts and relies instead on the movement or a property change of a fluid contained in the waveguide microchannels [1, 2]. Microfluidic optical switches utilizing similar concepts were developed by Agilent Technologies Inc. [2]. The fluid-based switch consists of intersecting silica waveguides, with trenches etched diagonally at each point of intersection. The trenches contain an index-matching fluid that in default mode allows transmission of light unimpeded through the switch. To switch the light path, bubbles are formed and removed hundreds of times per second in the fluid using a thermal actuator. The bubbles reflect the light from the input waveguide to the output waveguide.

Silicon microfabrication technologies are dominant in the manufacturing of switch waveguide. Simplifying the fabrication process, laser microprocessing technique offers the means for a flexible, short lead time, low cost and reliable method. Laser assisted chemical etching has succeeded in fabricating waveguides in glass [3]. However, the ultrashort pulse lasers have made it feasible to directly machine microchannels and create waveguides in materials of interest [4]. The femtosecond laser pulses present extremely high peak power and produce nearly no thermal damage as the pulse duration is shorter than the thermalization time (of order of 10 picoseconds) [5]. Compared with the long pulse lasers and other conventional fabrication technologies, femtosecond laser tools show great promise for the precise control of material removal with negligible thermal damage and the absence of a liquid phase during material removal. Also, the laser can be used to process a wide range of materials and have the capability to fabricate feature sizes in micro scales. X-ray Diffractometer (XRD) analysis of the femtosecond laser-

H.Y. Zheng (✉) · H. Liu · S. Wan · G.C. Lim
Singapore Institute of Manufacturing Technology,
71 Nanyang Drive, Singapore 638075
E-mail: hyzheng@simtech.a-star.edu.sg
Tel.: +65-6793-8504
Fax:+65-6792-2779

S. Nikumb · Q. Chen
Integrated Manufacturing Technologies Institute,
National Research Council of Canada,
800 Collip Circle, London, Ontario N6G 4X8, Canada

processed shape memory alloys has already supported the belief of nonthermal machining [6].

In this work, transparent polymer and glass substrates were studied to demonstrate laser micro machining of high quality microchannels for use as bubble switches for optical signals. Since diode laser pumped solid-state lasers are known for their compactness and ease of use, our research on machining aluminosilicate glasses included comparative results using a nanosecond pulse Nd:YAG laser, in addition to the femtosecond laser. The preliminary testing of the switch design concept, based on the thermo-capillary effect, was carried out on with the refractive index-matching liquid. The testing was successful in confirming the working principle of the device.

2 Experimental arrangement

The experimental setup is shown in Fig. 1. The femtosecond laser (CPA-2001, Clark-MXR Inc.) operates with a pulse width of 150 fs at a fundamental wavelength of 775 nm. A 1/4 waveplate was used to change the p-polarized beam into a circularly polarized beam. The focal length of the focusing lens was 50 mm. The repetition rate was adjustable to 1 kHz and a stream of N_2 gas was blown sideways to the cutting direction in order to reduce the material redeposition. The surface morphology of the machined channels was investigated with a scanning electron microscopy (SEM) and roughness measurements were performed with a Taylor Hobson surface profiler and a Wyko NT3300 (Veeco Metrology Group) interferometer. A compact DPSS nanosecond pulse laser (AVIA, Coherent Inc.) was also used for laser micromachining of glass. The laser was operated in Q-switched mode with TEM_{00} output at 355 nm.

Two materials were studied: a commercial polycarbonate (4 mm in thickness) and aluminosilicate glasses sheet (0.15 mm in thickness, MATSUNAMI Glass). All the samples were cleaned by ultrasonic cleaning at 40 °C for 30 minutes before and after laser processing.

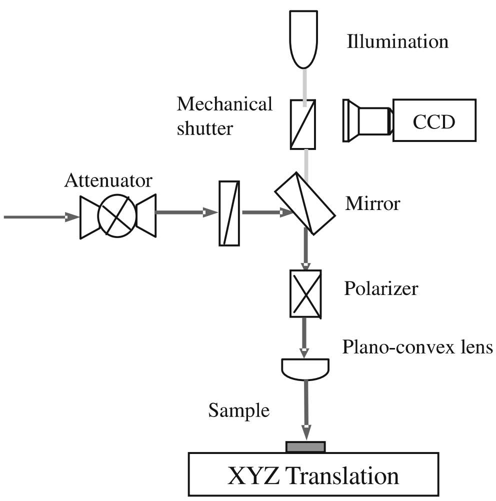

Fig. 1. The schematic of the experimental setup

3 Micromachining with a femtosecond laser

Studies were focused on achieving microchannels with good surface finishing. Microchannels of 160 μm in width were fabricated using four beam passes with varying center-to-center distance (at 40 μm that corresponds to approximately the effective beam size on the substrate surface) as illustrated in Fig. 2. The other processing variables investigated were cutting speed, power density, and repetition rate of the given materials.

3.1 Cutting speed vs. surface roughness

The correlation between the cutting speed and the surface roughness (Ra) is shown in Fig. 3. The laser power density and the repetition rate were set at 4×10^3 W/cm^2 and 1000 Hz, respectively.

It is seen that the surface roughness (Ra) was decreased rapidly from 426 and 155 nm for the PC and glass materials, respectively, to about 60 nm when the cutting speed was increased from 0.050 mm/s to 0.200 mm/s and decreased more gradually afterwards. Ridges in the microchannel between the beam paths were observed, which contributed to the surface roughness as the measurement was conducted across the ridges. In fact, the calculated number of pulses per site was shown to decrease rapidly at the slower speeds (more pulses and thus deeper cuts) and much more gradually at the higher speeds (less pulses and thus shallower cuts). This explains the changed pattern in the measured surface roughness (Ra).

3.2 Power density vs. surface roughness

The effect of the power density on the surface roughness was investigated as shown in Fig. 4. The cutting speed and repetition rate were fixed at 0.2 mm/s and 1000 Hz, respectively.

Fig. 2. Laser beam path for the machining of microchannels

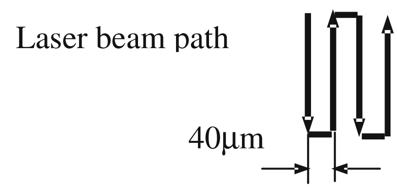

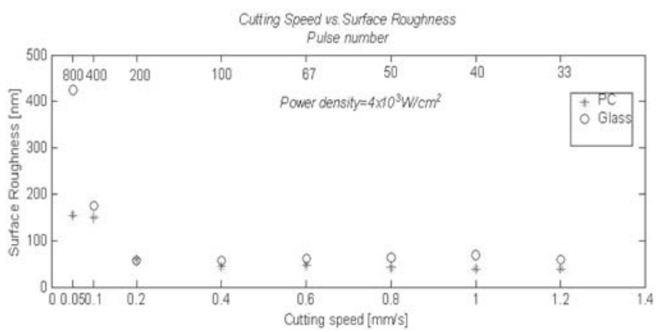

Fig. 3. Cutting speed vs. surface roughness, and femtosecond laser: 4×10^3 W/cm^2 and 1000 Hz

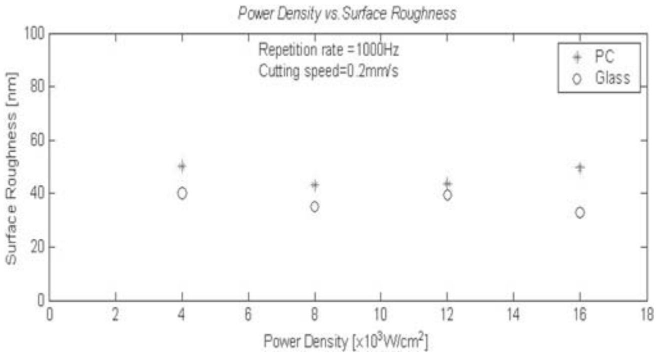

Fig. 4. Effect of power density on the surface roughness

It can be seen that the surface roughness (Ra) of both polycarbonate and the glass remained almost the same at 50 nm and 40 nm, respectively, when the power density was varied between 4×10^3 W/cm^2 and 16×10^3 W/cm^2. The four times increase in power density did not result in significant thermal effect that often leads to rougher surfaces.

This result is different from what is normally observed in longer pulse laser machining, where excessive power causes heat diffusion into the adjacent materials leading to rougher surfaces due to the thermal effect. With the femtosecond pulses, heat diffusion was found to be negligible.

3.3 Repetition rate vs. surface roughness

As discussed earlier, ultrashort pulse laser processing is believed to be nonthermal processing with minimal thermal effects (i.e., absence of melting and thermally induced cracks). However, it has been speculated that the thermal effect may become noticeable due to the accumulation of pulses at high repetition rates – a phenomenon often observed in excimer laser processing.

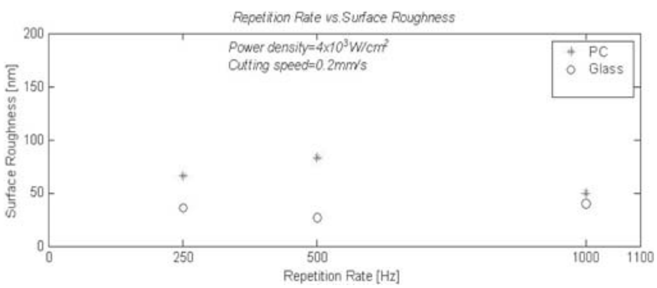

Fig. 5. Effect of repetition rate on surface roughness at power density of 4×10^3 W/cm^2

A study was thus carried out to understand the heat accumulation effect by varying the repetition rate of the femtosecond laser. The power density was set at 4×10^3 W/cm^2 and the cutting speed was set at 0.20 mm/s. The result is shown in Fig. 5. For polycarbonate, the surface roughness (Ra) was measured as 0 nm, 80 nm, and 40 nm at the repetition rates of 250 Hz, 500 Hz, and 1000 Hz, respectively. For the glass substrate, the surface roughness (Ra) was 40 nm, 30 nm, and 40 nm at the repetition rates of 250 Hz, 500 Hz, and 1000 Hz, respectively. The relatively small variation in Ra is believed to be due to the measurement errors. If there was melting due to the accumulated thermal effect at the higher repetition rates, the surface roughness, particularly for the glass material, should have been lower. Therefore, the heat accumulation effect at higher repetition rates was not observed.

3.4 Topography

An example of the laser-cut microchannel in the polycarbonate material is shown in Fig. 6. The power density was set at 8×10^3 W/cm^2, the cutting speed was at 0.1 mm/s, and the repetition rate was 1000 Hz. It can be seen that the ridges formed at the bottom due to the beam overlaps. However, the sidewalls were smooth and straight.

An example of the femtosecond laser-cut microchannel in the aluminosilicate glass is also shown in Fig. 7. The SEM micrographs of Figs. 7a and 7b provide the surface topography and the cross section of the glass microchannel machined at the power density of 4×10^3 W/cm^2 and the speed of 0.1 mm/s. No melting or microcracks were observed. The microchannel is however not straight and has an uneven bottom surface. To make more straight channels, a thin glass was cut through at a power density of 16×10^3 W/cm^2, speed of 0.1 mm/s, and repetition rate of 1000 Hz as shown in Fig. 7c. The bottom surface roughness was below 100 nm, which was appropriate for the prototype fabrication of the microfluidic switching device.

Machining of the aluminosilicate glasses using a 3rd harmonic Nd:YAG laser was also performed. By carefully selecting

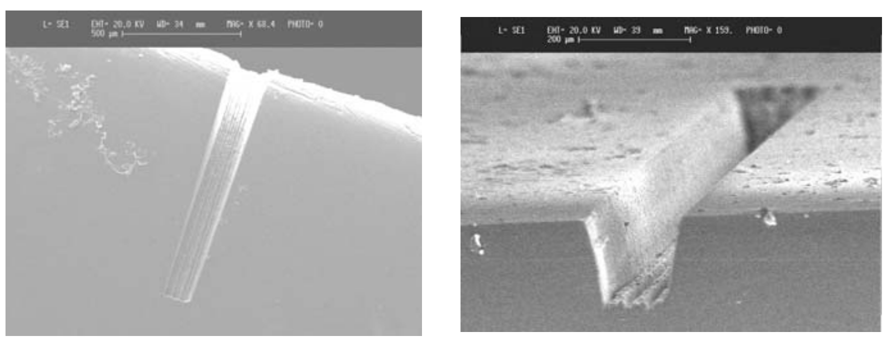

(a) (b)

Fig. 6a,b. SEM micrographs of polycarbonate microchannels machined by the femtosecond laser at 8×10^3 W/cm^2, speed of 0.1 mm/s, and repetition rate of 1000 Hz **a** top view **b** cross section view

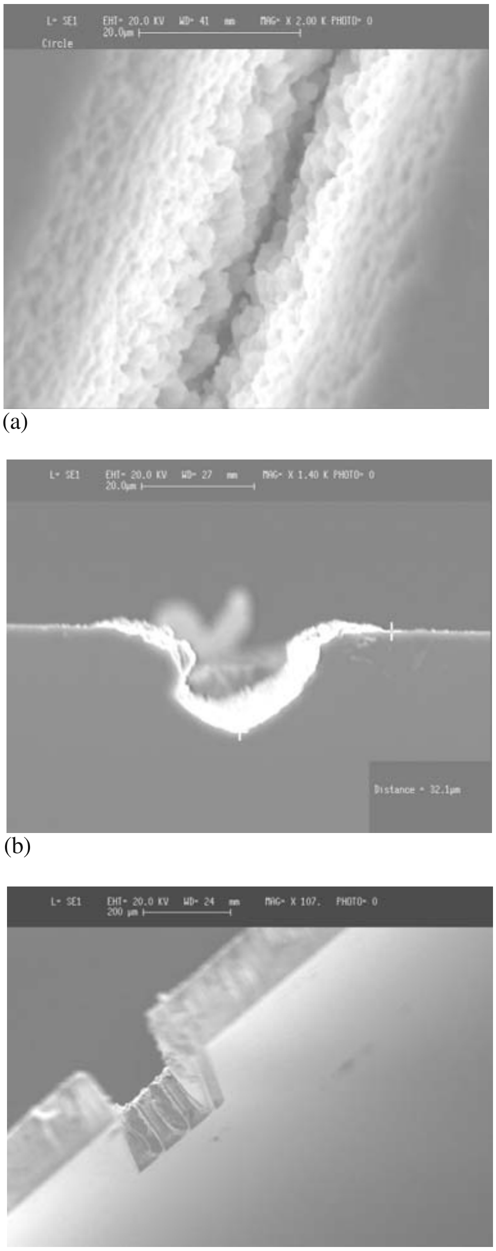

Fig. 7a–c. SEM micrographs **a** the surface topography **b** cross section of the aluminosilicate glass microchannel **c** side wall of the cut-through channel machined by the femtosecond laser

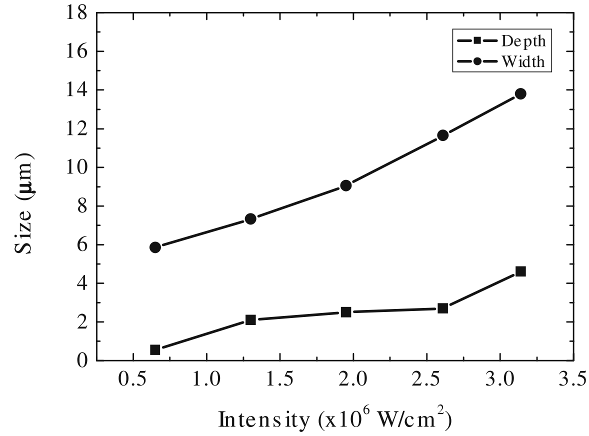

Fig. 9. Relationship between the depth and width of the microchannels and the laser intensity under optimal conditions for fabrication in aluminosilicate glass by a frequency-tripled YAG laser

the experimental processing parameters such as wavelength, intensity, repetition rate, sample surfaces, scanning rate, etc., high quality, crack-free laser micromachining on glass material can be achieved. Figure 8 shows the fabricated microchannels on the glass surface under the best focusing and defocusing conditions and an example of a machined microchannel under optimal conditions with laser intensity of 1.30×10^6 W/cm^2. The relationship between the depth and width of the microchannels and the laser intensity for optimal condition was plotted in Fig. 9. Control of the groove width can be realized by careful adjustment of the laser intensity. The mounds produced at the edges of the microchannels can be removed using suitable chemical treatment, e.g., dilute HF solution. However, to avoid any influence from additional factors, such treatment was not used.

4 Preliminary design of a bubble switch

A microfluidic optical bubble switch, suitable for the integration with the optical waveguide on substrate, was designed and fabricated for preliminary testing. The switching mechanism is based on the thermocapillary effect induced by the temperature gradient across the microchannel. The switch consists of an oil-filled microchannel with a pair of microheaters. To shorten the switching time, some design considerations were proposed and

Fig. 8a,b. Microchannels machined in aluminosilicate glass fabricated by a frequency-tripled diode-pumped YAG laser **a** machining under the best focusing and defocusing conditions **b** machining under the best focusing condition with laser intensity of 1.30×10^6 W/cm^2

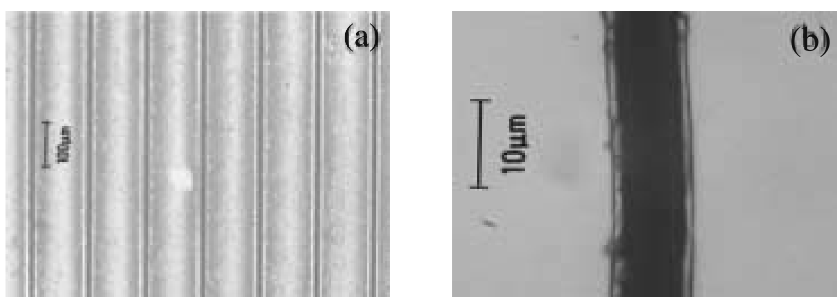

identified through experimentation. The prototype was fabricated in polymer and glass materials, respectively, by the femtosecond laser micromachining.

4.1 Conceptual and structural design

Figure 10 shows the thermocapillary switch consisting of an intersecting waveguide substrate, in which there is a microchannel full of index-matching liquid at the junction. It is a so-called bubble-driven type switch because a bubble is located in the microchannel and surrounded by the index-matching liquid. This switch is based on the total internal reflection principle, resulting from the air bubbles in a capillary channel reported by Jackel and Tomlinson [7] in 1990.

When the bubble moves away from the junction, the optical signal propagates straight through the slit (Fig. 11a). When the bubble is present at the junction of the waveguide, the optical signal switches into the junction waveguide through the total internal reflection on the channel sidewall as depicted in Fig. 11b.

Two microheaters were located at both sides of the microchannel to produce a temperature gradient along the channel. The bubble is driven toward the higher temperature region that is caused by the surface tension of the air-liquid interface, an effect known as thermocapillary effect [1].

To shorten the switching time, one way is to minimize the heat transfer time between the microheaters and the refractive index-matching fluid. Therefore, one slot was deposited with a thin aluminum layer to connect the heaters and the fluid channel was fabricated to transfer the heat faster than the substrate. Another way is to fabricate the microchannel into two sections. A small ridge was formed at the center to stop the bubble. It reduces half of the traveling distance of the bubble and stabilizes the bubble movement at the junction point.

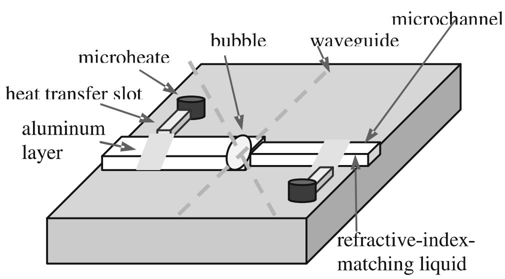

Fig. 10. The thermocapillary bubble switch structure

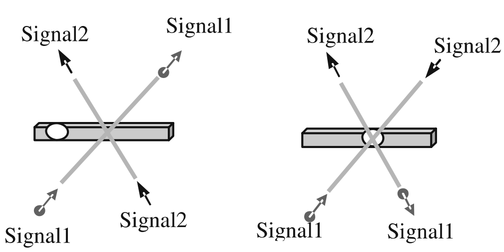

Fig. 11a,b. Bubble switch operation principle **a** index fluid at the waveguide junction "off" state **b** bubble at the waveguide junction "on" state

4.2 Preliminary testing result

Dimethylphenylmethylsiloxane was chosen as the refractive index-matching liquid for the bubble switch because it has high thermal stability and low volatility and also because the refractive index can be adjusted by changing the mixtures of the dimethyl and diphenyl chemicals [7].

A prototype was fabricated in a glass substrate by the femtosecond laser micromachining. The dimension of the fluid channel was about 0.2 mm $(W) \times 0.15$ mm $(H) \times 20$ mm (L). The gap between the heat resistors and the fluid channels was 0.5 mm. The air bubble was injected into the fluid channel by a syringe. The substrates were sealed by epoxy resin.

It was observed that the air bubble moved along the channel driven by the surface tension, as a result of the temperature gradient generated due to microheaters. Although it took 2 to 3 seconds for the bubble to reach the junction point, the prototype proved the conceptual design principle. It is anticipated that the proposed method of shortening the switching time as well as ultrafine microchannel designs will provide the desired milliseconds switching time.

5 Conclusions

The effect of the short pulse laser machining parameters such as cutting speed, repetition rate, and the power density on the surface quality of polycarbonate and aluminosilicate glass materials were investigated. Microchannels with bottom surface roughness of around 40 nm have been fabricated.

The conceptual preliminary design of a thermocapillary bubble switch was realized and tested on the glass substrate material. Further development is needed to shorten the switching time.

Acknowledgement The authors would like to thank Dr. Xiong ZhengJun and Dr. Qiu Hong for their valuable discussions. This material is based on the work supported by the Agency for Science, Technology and Research, Singapore, under grant number 172/4/4-10V1.

References

1. Makihara M, Sato M (1999) Micormechanical optical switches based on thermocapillary integrated in waveguide substrate. Lightwave Technol 17(1):14
2. Ware A (2000) New photonic-switching technology for all-optical networks. Lightwave, March 2000, pp 92–98
3. D'Aubigny CYD, Walker CK, Jones BD (2001) Laser microchemical etching of waveguides and quasi-optical components. Proc SPIE 4557:101–110
4. Bado P (2000) Ultrafast pulses create waveguides and microchannels. Laser Focus World 36(4):73–78
5. Stuart BC, Feit MD, Herman S, Rubenchik AM, Shore BW, Perry MD (1996) Nanosecond-to-femtosecond laser-induced breakdown in dielectrics. Phys Rev B 53(4):1749–1761
6. Zheng HY, Zareena AR, Huang H, Lim GC (2003) Studies of femtosecond laser-processed Nitinol. J Mater Sci Forum 437–438:277–280
7. Jackel JL, Tomlinson WJ (1990) Bistable optical switching using electrochemically generated bubbles. Opt Lett 15(24):1470